CHEMISTRY
A EUROPEAN JOURNAL

DOI: 10.1002/chem.200500926

Synthesis and Some Properties of Binuclear Ruthenocenes Bridged by Oligoynes: Formation of Bis(cyclopentadienylidene)cumulene Diruthenium Complexes in the Two-Electron Oxidation

**Masaru Sato,*[a] Yusuke Kubota,[a] Yasushi Kawata,[a] Takashi Fujihara,[a]
Kei Unoura,[b] and Aiko Oyama[b]**

Abstract: The monoynes $[Rc^*C{\equiv}CRc^*]$ and $[Rc'C{\equiv}CRc']$ were obtained in improved yields using $[Mo(CO)_6]$/2-FC_6H_5OH as a catalyst in the alkyne metathesis of $[Rc^*C{\equiv}CMe]$ and $[Rc'C{\equiv}CMe]$, respectively (Rc = ruthenocenyl, Rc* = 1″,2″,3″,4″,5″-pentamethylruthenocenyl, and Rc′ = 2′,3′,4′,5′-tetramethylruthenocenyl groups). The diynes $[Rc^*(C{\equiv}C)_2Rc^*]$ and $[Rc'(C{\equiv}C)_2Rc']$ were synthesized by the oxidative coupling of the corresponding terminal ethynes in good yields. The triyne $[Rc^*(C{\equiv}C)_3Rc^*]$ and the tetrayne $[Rc^*(C{\equiv}C)_4Rc^*]$ were prepared by the hetero- and homocoupling of $[Rc^*C{\equiv}CC{\equiv}CH]$, which was obtained from the reaction of $[Rc^*C{\equiv}CCHO]$ with $Li[N_2CSiMe_3]$, respectively. Although the oxidation waves did not always exhibit a clear two-electron oxidation process, the oxidation potentials shifted to a lower potential with an increase in the number of methyl substituents on the ruthenocenyl ring, and shifted to a higher potential with the increase in the number of C≡C units; this result is in contrast to that found in the $[Rc(CH{=}CH)_nRc]$ series. The chemical oxidation of $[Rc'C{\equiv}CRc']$ yielded a stable two-electron-oxidized species, the structure of which was confirmed by X-ray crystallography to be $[Ru_2(\mu_2\text{-}\eta^6{:}\eta^6\text{-}C_5Me_4C{=}CC_5Me_4)(\eta\text{-}C_5H_5)_2](BF_4)_2$. Changing the substituents (Rc, Rc*, and Rc′) had no effect on the chemical oxidation, but in the case of the Rc′ series the Me substituent increased the stability of the two-electron-oxidized species in solution. The diyne $[Rc^*(C{\equiv}C)_2Rc^*]$ and the triyne $[Rc^*(C{\equiv}C)_3Rc^*]$ also gave a similar but unstable two-electron-oxidized species. In acetone or acetonitrile, the two-electron-oxidized species of $[Rc^*C{\equiv}CRc^*]$ and $[Rc^*(C{\equiv}C)_2Rc^*]$ gradually formed the corresponding bis(fulvene)-type complexes. This implies that the two-electron-oxidized species of $[Rc^*(C{\equiv}C)_nRc^*]$ are destabilized with the increasing *n*.

Keywords: alkyne ligands · cumulenes · metallocenes · oxidation · ruthenium

Introduction

Much attention has been focused on the investigation of the electronic communication between metal centers, for the developing of functionalized materials with potential use as organometallic carbon rods, molecular wires, or electronic devices.[1,2] In the field of organometallics, dinuclear ferrocene derivatives that provide a two-step one-electron redox system have been extensively studied from the viewpoint of mixed-valence complexes.[3,4] Recently, a variety of dinuclear transition-metal complexes bridged by unsaturated organic compounds have been reported. Of these, μ-C-bridged binuclear complexes have attracted considerable attention as a fundamental class of carbon-rich molecular wires.[5–21] Most of the complexes have been shown to undergo consecutive one-electron redox reactions.[6,7,9,13,14,17–21] On the other hand, a few dinuclear transition-metal complexes have been found in which no one-electron oxidized species could be detected and an interesting structural rearrangement of the ligands occurred.[22–25] Recently, we have found that the dinuclear ruthenocene derivatives bridged by unsaturated organic compounds have shown one-step two-electron redox behavior. For example, biruthenocene,[26] 1,2-bis(ruthenocenyl)ethenes,[27] and 1,2-bis(ruthenocenyl)ethynes[28] under-

---

[a] Prof. M. Sato, Y. Kubota, Y. Kawata, Prof. T. Fujihara
Department of Chemistry, Faculty of Science
Saitama University, Saitama
Saitama 338–8570 (Japan)
Fax: (+81) 48-858-3700
E-mail: msato@chem.saitama-u.ac.jp

[b] Prof. K. Unoura, A. Oyama
Department of Chemistry, Faculty of Science
Yamagata University, Kosirogawa
Yamagata 990–8560 (Japan)

went two-electron oxidation to generate a product with a remarkable structural rearrangement. It has been found that the bridging chain length influences the electron communication in the successive one-electron redox system in $[Cp^*(NO)(Ph_3P)Re(C{\equiv}C)_nRe(PPh_3)(NO)Cp^*]$ (Cp^* = pentamethylcyclopentadienyl),[6e,f] $[Cp^*(dppe)Fe(C{\equiv}C)_nFe(dppe)Cp^*]$ (dppe = 1,2-bis(diphenylphosphino)ethane),[7c,f] $[C_6F_5\{(p\text{-}Tol)_3P\}_2Pt(C{\equiv}C)_nPt\{P(p\text{-}Tol)_3\}C_6F_5]$ (*p*-Tol = *para*-tolyl),[14c] $[Fc(CH{=}CH)_nFc]$ (Fc = ferrocenyl),[29] and $[FcPhC{=}(C{=})_nCFcPh]$.[30] These investigations lead to our interest on the effect of the bridging chain length on the oxidative behavior and the properties of their two-electron-oxidized species of the dinuclear ruthenocenes bridged by an unsaturated carbon chains. The biruthenocenes bridged by an oligoene have been confirmed to be a one-step two-electron redox system with chemically reversible reactions.[31] The oxidation potential in the series shifted to a lower potential with the increase in the number of ethene bonds and the two-electron-oxidized species were stable despite the bridging length. Herein, we report the synthesis and redox properties of the biruthenocenes bridged by mono-, di-, tri-, and tetraynes, and the related chemistry.

Results and Discussion

Synthesis and structural assignment: It has been reported that complex $[RcC{\equiv}CMe]$ (**1**) was refluxed with 10 mol% of $[Mo(CO)_6]$ and $p\text{-}ClC_6H_4OH$[32] in toluene for 2 h to give $[RcC{\equiv}CRc]$ (**4**) in good yield, but the similar reaction of $[Rc^*C{\equiv}CMe]$ (**2**) and $[Rc'C{\equiv}CMe]$ (**3**) gave the corresponding alkyne derivatives, $[Rc^*C{\equiv}CRc^*]$ (**5**) and $[Rc'C{\equiv}CRc']$ (**6**), in yields of only 11 and 3% yields, (Rc = ruthenocenyl, Rc* = 1″,2″,3″,4″,5″-pentamethylruthenocenyl, Rc′ = 2′,3′,4′,5′-tetramethylruthenocenyl) (Scheme 1).[28] The use of 20 mol% of the catalyst in the reaction of **2** improved the yield of **5** to 38%. However, a similar increase of the catalyst in the reaction of **3** did not improve the yield of **6**; instead colorless crystals of **7** (Scheme 2) were produced as the main product (76%). In the ^{1}H NMR spectrum of **7**, the Me signal at $\delta = 1.66$ ppm was observed as a broad singlet at room temperature and as a doublet at 60°C; the olefin proton signal appeared as a quartet at $\delta = 5.26$ ppm. Based on the ^{1}H NMR and H,H-COSY spectra, the structure of **7** was assigned to $[Rc'(p\text{-}ClC_6H_4O)C{=}CH(CH_3)]$, as shown in Scheme 2, and was confirmed by X-ray diffraction. This is a novel example of a 1,2-addition of a phenol group to a triple bond, although the reaction mechanism is unknown. The crystallographic data for **7** are listed in Table 1 and the selected bond lengths and angles are summarized in Table 2. The ORTEP view of **7** is shown in Figure 1. The olefinic plane is declined by 61.63(3)° from the plane of the Rc′ η-C_5Me_4 ring, probably because of the steric repulsion between the Rc′ group and the chlorophenoxyl group. The

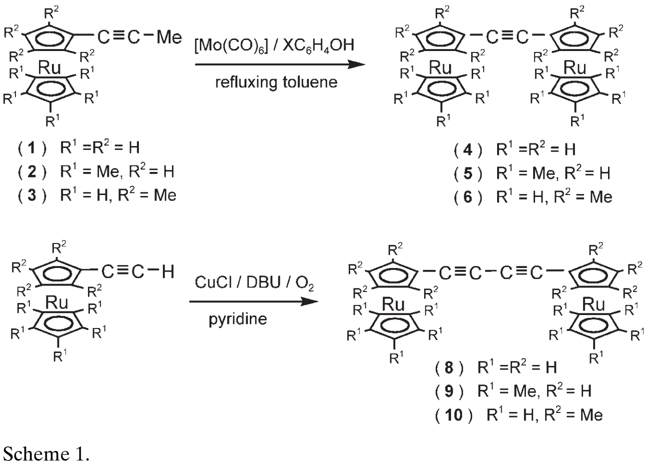

Scheme 1.

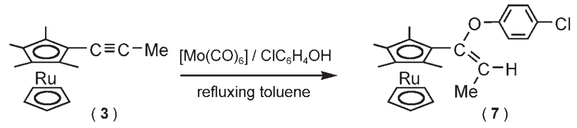

Scheme 2.

Table 1. Crystallographic data for **7** and **19**.

	7	**19**
formula	$C_{23}H_{25}ClORu$	$C_{30}H_{34}B_2F_8Ru_2$
M_r	453.975	770.33
crystal system	triclinic	monoclinic
space group	$P\bar{1}$	$P2_1/n$
a [Å]	8.7890(4)	7.6768(15)
b [Å]	9.9120(5)	13.159(3)
c [Å]	12.3140(7)	15.404(3)
α [°]	76.357(3)	
β [°]	83.962(3)	90.43(3)
γ [°]	87.401(2)	
V [Å^3]	1036.47(9)	1556.0(5)
Z	2	2
ρ_{calcd} [Mg m^{-3}]	1.455	1.644
crystal size [mm]	0.50x0.08x0.08	0.31x0.22x0.21
index limits	$-11 \leq h \leq 11$, $-12 \leq k \leq 12$ $-15 \leq l \leq 15$	$-8 \leq h \leq 10$ $-17 \leq k \leq 16$ $-20 \leq l \leq 20$
reflns measured	6342	11413
unique reflns	3963	3853
μ [mm^{-1}]	0.894	1.037
reflns used	3963	3853
parameters	235	194
R	0.0477	0.0378
wR	0.1241	0.1023
S	1.217	1.036
max/min peak in final map [e Å^{-3}]	0.507/−1.033	0.762/−0.516

Table 2. Selected bond lengths [Å] and bond angles [°] for **7**.

C1−C15	1.477(5)	C15−C16	1.328(6)
C16−C17	1.455(7)	C15−O1	1.389(5)
O1−C18	1.385(5)	Ru1−CCp	2.162(av.)
CCp−CCp	1.398(av.)		
C1-C15-C16	124.7(3)	C15-C16-C17	126.6(4)
O1-C15-C16	124.6(4)	C15-O1-C18	121.1(3)
C2-C1-C15	124.5(3)	C5-C1-C15	127.1(3)

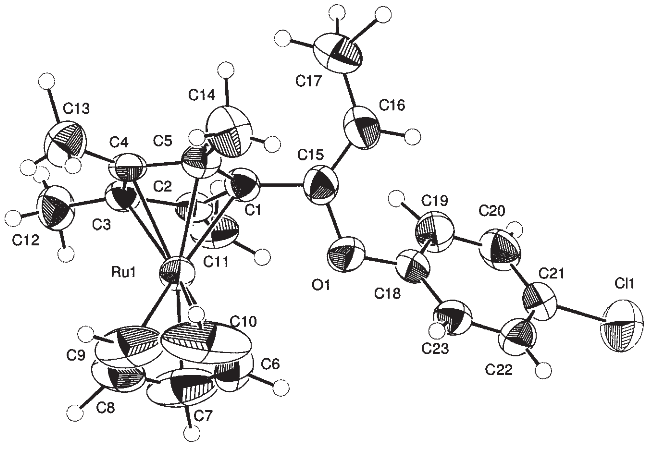

Figure 1. ORTEP view for complex **7**.

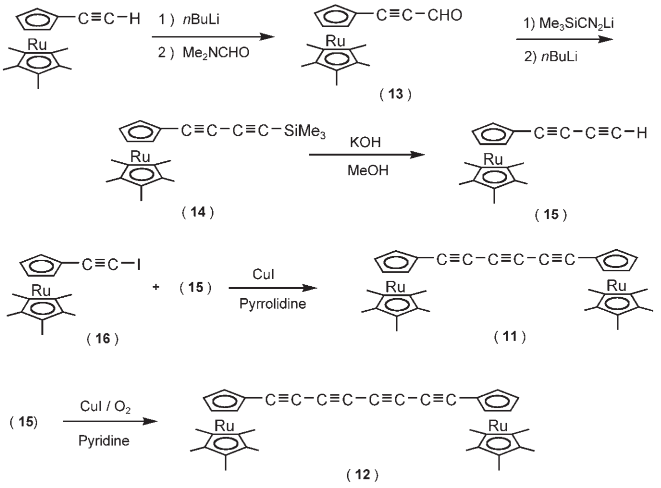

Scheme 3.

plane of the benzene ring of the chlorophenoxyl group also deviates from the olefinic plane by 59.10(3)°. The use of 2-FC_6H_4OH[33] instead of p-ClC_6H_4OH in the alkyne metathesis of **2** greatly improved the yield of **5** (60%). The similar reaction of **3** led to the formation of [Rc′C≡CRc′] (**6**) in 22% yield.

It has been reported[34] that [RcC≡CC≡CRc] (**8**) was obtained in good yield through the oxidative coupling of [RcC≡CH] using CuI/O_2 in pyridine. However, the oxidative coupling of [Rc*C≡CH] and [Rc′C≡CH] under similar conditions did not produce the corresponding diynes in high and reproducible yields. The diynes [Rc*C≡CC≡CRc*] (**9**) and [Rc′C≡CC≡CRc′] (**10**) were obtained in good yields by using $CuCl/DBU/O_2$ in pyridine (Scheme 1). Use of a strong base (DBU) is probably necessary because of the electron-donating properties of the methyl-substituted ruthenocenyl groups.

The triyne [Rc*C≡CC≡CC≡CRc*] (**11**) and the tetrayne [Rc*C≡CC≡CC≡CC≡CRc*] (**12**) were synthesized as shown in Scheme 3. The ethyne [Rc*C≡CH] was lithiated with *n*BuLi and followed by treatment with dimethylformamide to give [Rc*C≡CCHO] (**13**) in 95% yield. The reaction of **13** with $LiC(N_2)SiMe_3$, which was prepared from $Me_3SiCH(N_2)$ and lithium diisopropylamide (LDA), below −78 °C, and the subsequent treatment of *n*BuLi produced [Rc*C≡CC≡CSiMe$_3$] (**14**) in good yield (95%). The desilylation of **14** gave the butadiyne [Rc*C≡CC≡CH] (**15**) in a quantitative yield, but was unstable in air at room temperature. The lithium acetylide prepared from [Rc*C≡CH] and *n*BuLi was treated with iodine to produce [Rc*C≡CI] (**16**) in good yield, although it was unstable on heating. The heterocoupling reaction of **15** and **16** with CuI in pyrrolidine led to the triyne **11** in 72% yield. The carbon signals for the triple bond of **11** appeared at $\delta = 65.15$, 65.93, and 71.24 ppm in the ^{13}C NMR spectrum. The homocoupling reaction of **15** with CuI/O_2 in pyridine produced the tetrayne **12** in 70% yield. Complex **12** showed the signals for the C≡C triple bond at $\delta = 64.62$, 65.09, 65.98, and 71.61 ppm in the ^{13}C NMR spectrum. The electronic spectra of **5**, **9**, **11**, and **12** are shown in Figure 2. Three characteristics stand out: with the increase in the number of C≡C units 1) the absorption bands shifted to a long-wavelength region, 2) the absorbance intensified, and 3) fine structure in the absorption band appeared. These features are in agreement with general observations of acetylene derivatives.

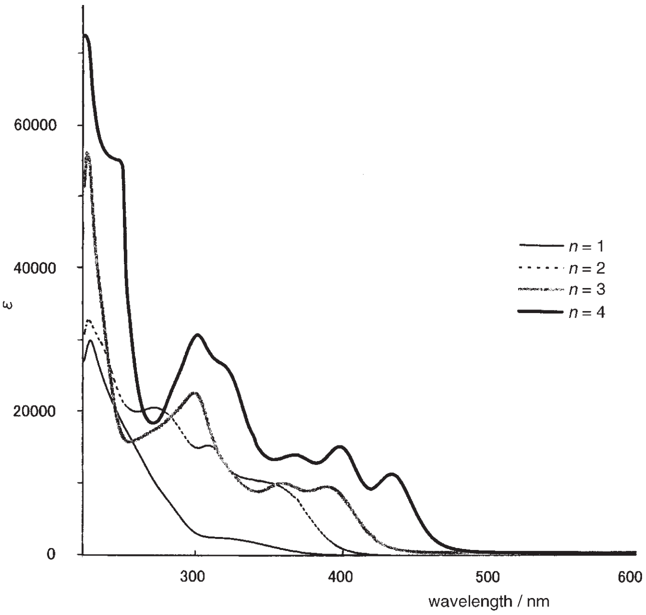

Figure 2. UV-visible spectra for [Rc*(C≡C)$_n$Rc*] (n=1: **5**, n=2: **9**, n=3: **11**, and n=4: **12**) in CH_2Cl_2.

Redox behavior: The cyclic voltammograms of monoynes **4**–**6**, diynes **8**–**10**, triyne **11**, and tetrayne **12** were measured in CH_2Cl_2. The cyclic voltammetry data of the oxidation potentials for these complexes are summarized in Table 3, along with those of the related complexes. The cyclic voltammo-

Table 3. Electrochemical data of [Rc(C≡C)$_n$Rc], [Rc′(C≡C)$_n$R′] (n=1–2), and [Rc*(C≡C)$_n$Rc*] (n=1–4) (in V vs FcH/FcH$^+$).

Complex	E_{pa} [V]	E_{pc} [V]	ΔE[a] [V]	i_{pc}/i_{pa}	n_{app}[b]
[RcC≡CRc] (**4**)	+0.39	+0.25(sh)	–	–	–[c]
		−0.03	–	–	
[Rc(C≡C)$_2$Rc] (**8**)	+0.53	+0.27	–	–	4.5±0.7
	–	+0.02	–	–	
[Rc*C≡CRc*] (**5**)	+0.09	−0.05	0.14	0.83	2.1±0.1
[Rc*(C≡C)$_2$Rc*] (**9**)	+0.26	+0.14	0.12	1.15	2.9±0.4
	+0.36	+0.22(sh)	0.14	–	4.3±0.5[d]
[Rc*(C≡C)$_3$Rc*] (**11**)	+0.37	+0.22	0.15	1.22	3.7±0.4
[Rc*(C≡C)$_4$Rc*] (**12**)	+0.39	+0.21	0.18	0.94	4.8±0.6
[Rc′C≡CRc′] (**6**)	+0.14	−0.02(sh)	0.14	–	2.0±0.3
	–	−0.23	–	–	
[Rc′(C≡C)$_2$Rc′] (**10**)	+0.27	+0.10	0.17	0.96	2.2±0.3
[RcC≡CMe] (**1**)	+0.50	+0.34	0.16	0.84	
[Rc*C≡CMe] (**2**)	+0.33	+0.17	0.16	0.66	
[Rc′C≡CMe] (**3**)	+0.35	+0.16	0.19	0.49	

[a] $\Delta E = E_{pa} - E_{pc}$. E_{pa} is the potential for an oxidation wave and E_{pc} is the potential for a reduction wave. [b] n_{app} is the apparent number of electrons involved in each step which is determined by the results of thin-layer coulometry for each oxidation peak. [c] The electron count could not be measured because of the insufficient solubility of the complex. [d] The electron count was obtained by the electrolysis after the second wave.

grams of **5**, **9**, and **11** are shown in Figure 3. As seen in Figure 3 and Table 3, the redox process of these complexes is not reversible, because the ΔE ($E_{pc} - E_{pa}$) is 0.15–0.20 V. Thin-layer coulometry gave the apparent electron counts (n_{app}) for the oxidation waves of **5**, **6**, and **8**–**12** (Table 3).

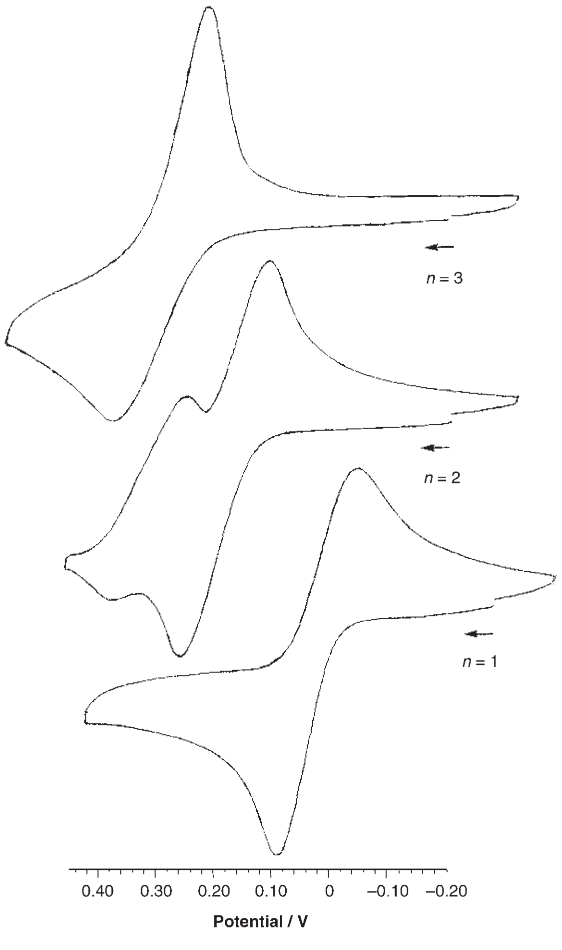

Figure 3. Cyclic voltammograms for **5** (bottom), **9** (middle), and **11** (top) in CH$_2$Cl$_2$ (sweep rate=0.1 Vs^{-1}, [complex]=0.5 mmol).

The complexes **5**, **6**, and **10** undergo two-electron oxidation at about 0.1–0.3 V. The cyclic voltammograms of **8**, **11**, **12** exhibit the oxidation peaks, which might be due to a four-electron transfer, at approximately 0.4–0.5 V. Two oxidation peaks were observed in the cyclic voltammogram of **9**, probably because the two-electron-oxidized species was not very stable (vide infra). Further, it is interesting to note that the cyclic voltammogram of **9** (middle of Figure 3) gives the first oxidation peak, which might be based on a three-electron-transfer process, at 0.26 V and the second oxidation peak, which might be caused by a one-electron-transfer process, at 0.36 V. The less precise electron counts and multiple-electron transfers (3e$^-$ and 4e$^-$) suggest that this electrochemical process is not as simple as that in the dinuclear ruthenocenes bridged by oligoenes, which showed a clear two-electron oxidation process.[31]

The oxidation potentials of monoynes and diynes showed a cathodic shift, as follows: **4** (+ 0.39 V)>**6** (+ 0.27 V)>**5** (+0.09 V), **8** (+0.53 V)>**10** (+ 0.27 V)>**9** (+0.26 V). The trend seems to reflect an increase in the number of electron-donating methyl groups on the cyclopentadienyl ring of the ruthenocenyl moiety. Also, the oxidation potentials of **4**–**6** are lower than those of the corresponding propynes (**1**–**3**), while the oxidation potentials of dinuclear ruthenocenes bridged by oligoynes are shifted to a higher potential with the increase in the number of ethyne bonds, for example, as follows: [Rc*C≡CRc*] (−0.09 V)<[Rc*(C≡C)$_2$Rc*] (0.29 V)<[Rc*(C≡C)$_3$Rc*] (0.37 V)<[Rc*(C≡C)$_4$Rc*] (0.39 V). A similar trend was observed in the Rc and Rc′ series: [RcC≡CRc] (0.39 V)<[Rc(C≡C)$_2$Rc] (0.53 V) and [Rc′C≡CRc′] (0.14 V)<[Rc(C≡C)$_2$Rc′] (0.27 V). This tendency is in sharp contrast with that observed in the oligoene-bridged dinuclear ruthenocenes, in which the oxidation potentials are shifted to a lower potential with the extension of conjugation.[31] The anodic shift of the oxidation potential in the present series may be caused by the decrease in the metal–metal interaction as the number of C≡C units increases, because a similar tendency was observed in the successive one-electron redox systems, for example, [Cp*(NO)(Ph$_3$P)Re(C≡C)$_n$Re(PPh$_3$)(NO)Cp*],[6e,f] [Cp*(dppe)Fe(C≡C)$_n$Fe(dppe)Cp*],[7c] and [Fc(C≡C)$_n$Fc],[29] in which the metal–metal interaction weakens as linker chains become longer.

Theoretical study: To elucidate the electrochemical properties and the electronic features of the preceding complexes, we performed a computational study on [Rc*C≡CRc*] (**5**), [Rc*$(C{\equiv}C)_2$Rc*] (**9**) and [Rc*$(C{\equiv}C)_3$Rc*] (**11**). The structures of the complexes were geometry optimized and the optimized structure of **5** is shown in Figure 4 as an example.

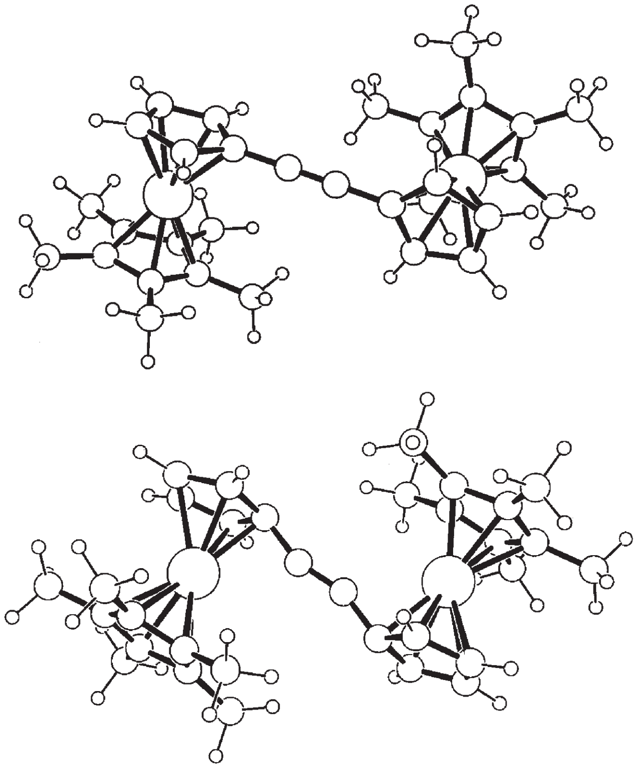

Figure 4. Optimized structure for **5** (top) and **18** (bottom).

The structural parameters obtained from the optimized structure of **5** are comparable with the crystallographically determined parameters for **5**.[28] The calculated C≡C (1.217 Å) and C−C (1.410 Å) bond lengths of the bridge are in good agreement with the observed distances (1.194(6) Å for the C≡C bond and 1.419(6) and 1.420(5) Å for the C−C bonds). The Ru−C (2.208 Å) and C−C (1.435 Å) distances in the Rc* moiety are also well reproduced (2.188 (av) and 1.429 Å (av) for the observed structure, respectively). In the optimized structure of **5**, the two Rc* groups are twisted by nearly 90° relative to each other around the linker. The twist conformation is more stable by 47.5 $kJ\,mol^{-1}$ than the anti conformation, in which the two Rc* groups are in an anti position to each other. The large energy difference may stem from the considerable overlap of the linker p orbital with both the Cp-ring p orbital and the Ru metal d orbital of the Rc* moiety in the HOMO of the twisted conformation, as seen in Figure 5; such an overlap was not seen in the anti conformation.

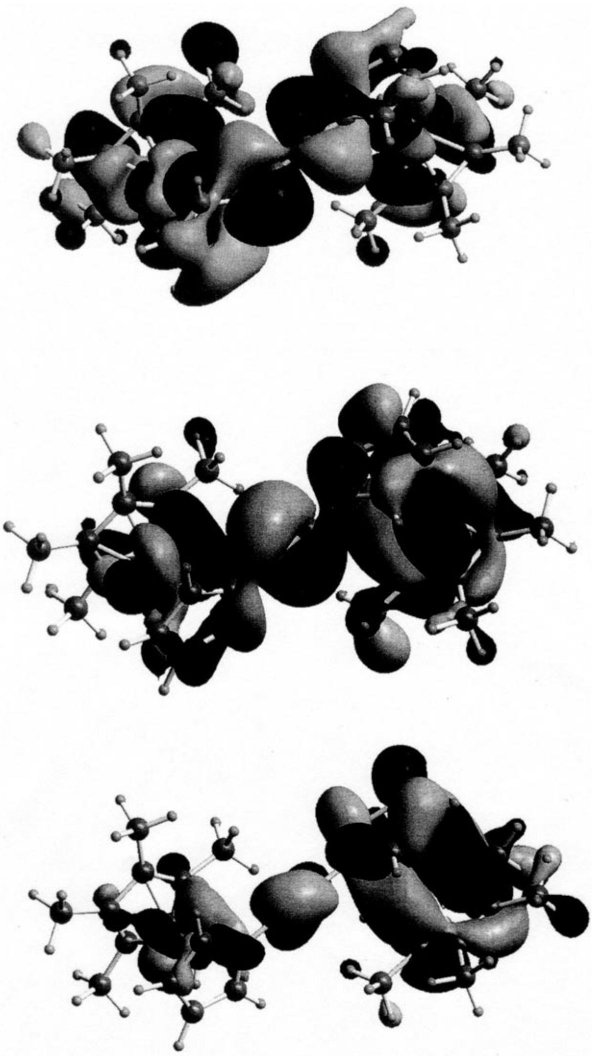

Figure 5. The graphic representation of the LUMO (top), HOMO (middle), and HOMO−1 (bottom) for the optimized structure of **5**.

In contrast with the Rc(CH=CH)$_n$Rc series, in which the energy of the HOMO increased with the increase in the number of CH=CH units,[31] the MO calculation in the [Rc*$(C{\equiv}C)_n$Rc*] series showed that the energy of the HOMO decreases in the following order: [Rc*C≡CRc*] (**5**) (−0.18273 a.u.) > [Rc*$(C{\equiv}C)_2$Rc*] (**9**) (−0.1859 a.u.) > [Rc*$(C{\equiv}C)_3$Rc] (**11**) (−0.18673 a.u.). On the other hand, the HOMO energy level of the oligoynes has been reported to increase with increased length in conjugation, for example, acetylene (Ip = 11.40 eV, Ip = ionization potential) and butadiyne (Ip = 10.17 eV). The same dichotomous trend was recently reported and rationalized in the computational investigation on the chain-length effects in diplatinum(II)–polyynediyl complexes and free polynenes.[35] If electrochemical oxidation is assumed to involve the removal of an electron from the HOMO, the descending order of the HOMO energy may explain the ascending order of the oxidation potentials in the [Rc*$(C{\equiv}C)_n$Rc*] series [**5** ($n=1$) (+0.09 V)[28] < **9** ($n=2$) (+0.26 V) < **11** ($n=3$) (+0.37 V)], although each oxidation process in these complexes may be somewhat different. The MO calculation also showed that the contribution of the metal d orbital to the HOMO dramatically decreases with the extension of the conjugation ($n = 1$, 67.6; $n = 2$, 55.1; $n = 3$, 22.2 %). This seems to imply that the interaction between the terminal metals decreases as the C≡C chain of the bridge becomes longer.

We also performed the MO calculation for the two-electron oxidized species of **4**, $[Rc^*C{\equiv}CRc^*]^{2+}$ (**18**), the optimized structure of which is shown in Figure 4. The optimized geometry for **18** reveals the following features:

1) The Rc* part adopts a fulvene-type structure, in agreement with the crystal structure; however, the Ru−C(α) (2.447 Å) and C(α)−C(ipso) (1.384 Å) distances for the optimized structure are somewhat longer than those for the observed structure (2.254(3) and 1.405(4) Å, respectively).[28]
2) The bridging carbon chain seems to behave like a cumulative bond; the center C−C bond length (1.273 Å) on the bridge is approximately the same as the mean length (1.27 Å) between the double and triple bonds and is similar to that observed.
3) The bridging carbon chain is no longer linear; the C(ipso)-C(α)-C(α′) angle (159.7°) is somewhat wider than the observed angle (153.5(3)°).
4) The C(α)−C(ipso) bond is folded at an angle of 34.2° from the η-C_5H_4 ring plane, the tilt angle is smaller than the value observed (41.3(3)°).

These features would suggest that the contribution of the fulvene structure to the oxidized species is smaller in the optimized structure than in the crystal structure. The features found in **18** were also observed in the two-electron-oxidized species (**19**) of [Rc′C≡CRc′] (vide infra). Thus, the MO calculations proved very helpful, allowing us to predict the structure of the oxidized species in the ruthenocene-terminated oligoyne series.

Chemical oxidation: It has been reported that the monoynes **4** and **5** were oxidized with *p*-BQ/$BF_3{\cdot}OEt_2$ (*p*-BQ = *para*-benzoquinone) to give stable two-electron-oxidized species, $[Ru_2(\mu_2\text{-}\eta^6{:}\eta^6\text{-}C_5H_4C{=}CC_5H_4)(\eta\text{-}C_5H_5)_2](BF_4)_2$ (**17**) and $[Ru_2(\mu_2\text{-}\eta^6{:}\eta^6\text{-}C_5H_4C{=}CC_5H_4)(\eta\text{-}C_5Me_5)_2](BF_4)_2$ (**18**), respectively.[28] When monoyne **6** was oxidized under similar conditions, the two-electron-oxidized species **19** was obtained as stable orange crystals (Scheme 4). The ^{1}H NMR spectrum of **19** showed only two signals for the methyl protons at $\delta = 2.04$ and 2.32 ppm, implying that **19** has a symmetric structure. In the ^{13}C NMR spectrum of **19**, the carbon signal on the bridging chain appeared at $\delta = 76.26$ ppm, similar to those found for **17** ($\delta = 77.67$ ppm) and **18** ($\delta = 80.10$ ppm). From these spectral data, the structure of **19** was assigned as $[Ru_2(\mu_2\text{-}\eta^6{:}\eta^6\text{-}C_5Me_4C{=}CC_5Me_4)(\eta\text{-}C_5H_5)_2](BF_4)_2$.

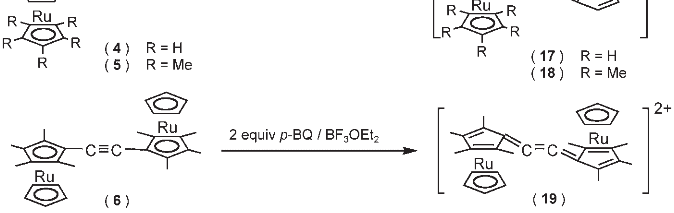

Scheme 4.

The structure of **19** was also confirmed by X-ray diffraction. The crystallographic data for **19** are listed in Table 1 and the selected bond lengths and angles are summarized in Table 4. The ORTEP view of **19** is shown in Figure 6; it shows that the bridging ligand is coordinated in the η^6-mode and in the anti configuration by two (η-C_5H_5)Ru groups. The Ru1−C1 distance is 2.178(3) Å, somewhat shorter than in $[Ru(\eta\text{-}C_5H_5)(\eta^6\text{-}C_5H_4CH_2)]^+$ (2.272(4) Å)[36]) and **18** (2.410 Å).[28] The C1−C2 bond is folded at an angle of 32.7° towards the η^4-C_5Me_4 ring; this value is considerably smaller than those for $[Ru(\eta\text{-}C_5Me_5)(\eta^6\text{-}C_5Me_4CH_2)]^+$ (40.3°),[37] $[Ru(\eta\text{-}C_5H_5)(\eta^6\text{-}C_5H_4CH_2)]^+$ (42.6°),[36] and **18** (41.3(3)°).[28] Also, the C1−C2 bond length (1.409(4) Å) is approximately the same as those of the fulvene complexes $[Ru(\eta\text{-}C_5Me_5)(\eta^6\text{-}C_5Me_4CH_2)]^+$ (1.401(4) Å)[37] and $[Ru(\eta\text{-}C_5H_5)(\eta^6\text{-}C_5H_4CH_2)]^+$ (1.405(5) Å).[36] The C1−C1 bond length (1.262(4) Å) is comparable to that of **18** (1.262(4) Å) and intermediate between the double- and triple-bond

Table 4. Selected bond lengths [Å] and bond angles [°] for **19**.

Ru1−C1	2.178(5)	Ru1−C2	2.067(3)
Ru1−C3	2.190(3)	Ru1−C4	2.264(3)
Ru1−C5	2.261(3)	Ru1−C6	2.184(3)
Ru1−C7	2.178(4)	Ru1−C8	2.192(4)
Ru1−C9	2.181(4)	Ru1−C10	2.214(3)
Ru1−C11	2.179(4)	C1−C1#	1.278(6)
C1−C2	1.409(5)	C2−C3	1.467(5)
C3−C4	1.416(5)	C4−C5	1.440(5)
C5−C6	1.412(4)	C2−C6	1.457(5)
$C(C_5H_5)-C(C_5H_5)$	1.395(av.)		
C1#-C1-C2	154.1(4)	C1#-C1-Ru1	139.5(3)
C1-C2-C3	114.7(3)	C1-C2-C6	115.3(3)
C3-C2-C6	109.7(3)	C2-C3-C4	105.3(3)
C3-C4-C5	109.5(3)	C4-C5-C6	109.8(3)
C5-C6-C2	105.7(3)	C1-C2-Cp'_{ctr}	33.7(2)

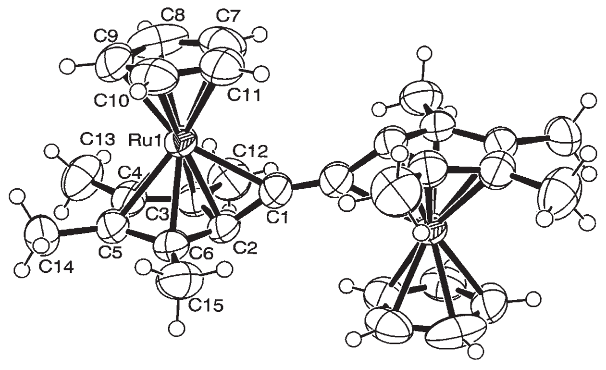

Figure 6. ORTEP view for complex **19**.

lengths. A clear bond alternation is observed in the C_5Me_4 ring of **19**. The angle C1-C1-C2 (154.1(4)°) is similar to that in **18** (153.5(3)°).[28] These data suggest that the dication of **19** can be regarded as a μ_2-bis(cyclopentadienylidene)ethene diruthenium complex. In the chemical oxidation of the mono-yne-bridged binuclear ruthenocenes, the methyl substituents have no effect, because **4**, **5**, and **6** all yield stable two-electron-oxidized species with similar structures.

The diyne **9** was oxidized in similar conditions to give a yellow-brown powder (**20**), which was unstable in solid form at room temperature, but was stable for few weeks at low temperatures. The dissolution of **20** in CD_3NO_2 generated a red-orange solution that remained stable below −20 °C. In the ^{1}H NMR spectrum of **20** in CD_3NO_2 at −20 °C, the chemical shift and signal pattern of the η-C_5H_4 ring protons were similar to those of **18**. The ^{13}C NMR spectrum showed the signals of the bridging carbon chain at $\delta = 78.53$ and 148.66 ppm, the latter of which was in the range observed in the cumulative bond of tetraphenylbutatriene ($\delta = 152.03$ ppm).[38] Based on these spectral data, the dication of **20** should be assigned to the μ_2-bis(cyclopentadienylidene)-butatriene diruthenium complex, $[Ru_2(\mu_2\text{-}\eta^6{:}\eta^6\text{-}C_5H_4C{=}C{=}C{=}CC_5H_4)(\eta\text{-}C_5Me_5)_2]^{2+}$, as shown in Scheme 5.

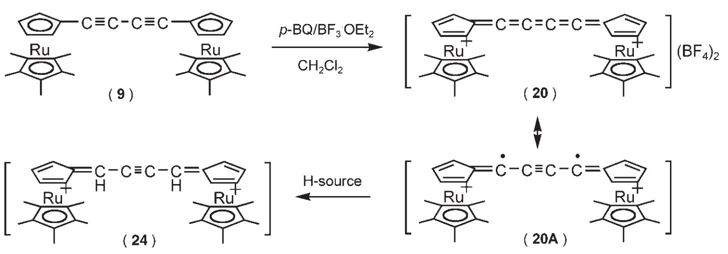

Scheme 5.

The oxidation of triyne **11** under similar conditions gave a yellow-brown powder (**21**) that was unstable at room temperature. Immediately after the isolation of **21** in CD_3NO_2, the ^{1}H NMR spectrum showed a chemical shift of the Me and η-C_5H_4 ring protons very similar to those of **18** and **20**, indicating the formation of a two-electron-oxidized species in which the two fulvene complexes are connected symmetrically by a cumulative bond. Therefore, it is supposed that the dication of **21** can also be formulated as the μ_2-bis(cyclopentadienylidene)hexapentaene diruthenium complex, $[Ru_2(\mu_2\text{-}\eta^6{:}\eta^6\text{-}C_5H_4C{=}C{=}C{=}C{=}C{=}CC_5H_4)(\eta\text{-}C_5Me_5)_2]^{2+}$. However, this species was highly unstable even in CD_3NO_2 at 0 °C, which gave rise to another set of peaks in the ^{1}H NMR spectrum (vide infra). The two-electron oxidized species of the tetrayne **12** gave no clear ^{1}H NMR spectrum in CD_3NO_2.

The solution of **18** in CD_3NO_2 was stable for several days at room temperature; however when it was dissolved in $(CD_3)_2CO$, it was gradually converted to $[Ru_2(\mu_2\text{-}\eta^6{:}\eta^6\text{-}C_5H_4CHCHC_5H_4)(\eta\text{-}C_5Me_5)_2]^{2+}(BF_4)_2$ (**22**). After 8 h, the ^{1}H NMR spectrum of **18** in $(CD_3)_2CO$ at room temperature showed new signals for the η-C_5H_4 ring protons at $\delta = 4.93$, 5.43, 5.86, and 5.98 ppm and for the olefinic proton at $\delta = 5.35$ ppm, as observed in **22**.[27] The formation of **22** from **18** in $(CD_3)_2CO$ may be elucidated as follows (Scheme 6). In **18**, there might be the contribution of the structure **18B** to a certain extent. If the biradical on the bridging ligand in **18B** abstracts a hydrogen atom from H_2O in the solvent, the formation of **22** can occur. These findings seem to indicate that some electrons can stay as a biradical on the bridging hydrocarbon as the result of spin uncoupling, as seen in the structure **18B**. The solution of **18** in CD_3CN showed a behavior similar to that in $(CD_3)_2CO$, but no generation of the Ru^{II}–Ru^{IV} mixed-valence complex **23** occurred, as it did for the two-electron-oxidized species of biruthenocene.[26] On the other hand, the dication **19** remained stable for several days in CD_3NO_2, CD_3CN, and $(CD_3)_2CO$, probably because of the steric protection of the methyl groups of the η-C_5Me_4 ligand.

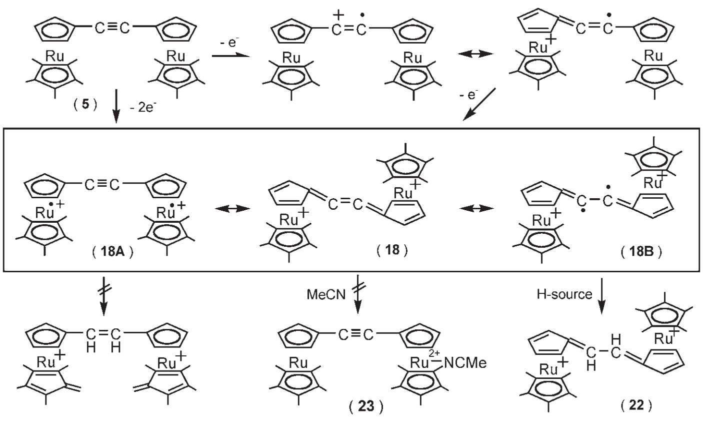

Scheme 6.

The ^{1}H NMR spectrum of **20** in CD_3NO_2 changed slowly at 0 °C. After 15 h, the signals due to the other product (**24**) were observed at about half the strength of that in **20**. In **24**, four η-C_5H_4 ring proton signals were observed, indicating an asymmetric environment, and their chemical shifts resembled those of **22**. Moreover, the ^{13}C NMR spectrum of **24** showed the one acetylene carbon signal at $\delta = 70.26$ ppm and the *exo*-carbon signal of the fulvene ligand at $\delta = 86.38$ ppm. These spectral data suggest that the dication of **24** is assignable to the bis(fulvene) complex $[Ru_2(\mu_2\text{-}\eta^6{:}\eta^6\text{-}C_5H_4CHC{\equiv}CCHC_5H_4)(\eta\text{-}C_5Me_5)_2]^{2+}(BF_4)_2$. The formation of **24** seems to be explained by the possibility that a biradical is generated at the 1,4-positions of the bridging carbon chain as the result of spin uncoupling (**20A**) (Scheme 5). Also, the minor component found in the ^{1}H NMR spectrum of **21** is suggested to be a higher analogue of **24**, namely $[Ru_2(\mu_2\text{-}\eta^6{:}\eta^6\text{-}C_5H_4CHC{\equiv}CC{\equiv}CCHC_5H_4)(\eta\text{-}C_5Me_5)_2]^{2+}(BF_4)_2$, because the ^{1}H NMR spectrum (the η-C_5H_4 ring protons at $\delta = 5.03$, 5.42, 5.56, and 6.17 ppm, and the methyl protons at $\delta = 2.25$ ppm) bears a close resemblance to that of **24**. These results indicate that a biradical can form on the bridging hydrocarbon of **18**, **20**, and **21** in solution and suggest that their two-electron-oxidized species cannot acquire enough resonance stability through the structural isomerization to a fulvene complex, which is caused by spin coupling. This finding is in sharp contrast to that observed in the oligoene bridged dinuclear ruthenocenes.[31]

Conclusion

Three new binuclear ruthenocene derivatives bridged by an oligoyne, $[\mathrm{Rc^*(C{\equiv}C)_{\mathit{n}}Rc^*}]$ ($n=2$–4), were prepared. The oxidation wave in $[\mathrm{Rc^*C{\equiv}CRc^*}]$ appeared at a remarkably low potential relative that in $\mathrm{Rc^*C{\equiv}CCH_3}$, and that in $[\mathrm{Rc^*(C{\equiv}C)_{\mathit{n}}Rc^*}]$ ($n=2$–4) showed an anodic shift with the increase in the number of C≡C units. This is in remarkable contrast to that observed in the case of $[\mathrm{Rc^*(CH{=}CH)_{\mathit{n}}Rc^*}]$, in which the oxidation wave shifted to the cathodic side. A MO calculation for the $[\mathrm{Rc^*(C{\equiv}C)_{\mathit{n}}Rc^*}]$ series showed that the energy of HOMO level decreased as the n value increased, which may be one of the reasons for the anodic shift of the oxidation potential. The optimized structure of the two-electron-oxidized species of $[\mathrm{Rc^*C{\equiv}CRc^*}]$ was in good agreement with X-ray structure in the dicationic complex **18**. The two-electron-oxidized species of $[\mathrm{Rc'C{\equiv}CRc'}]$ and $[\mathrm{Rc^*(C{\equiv}C)_{\mathit{n}}Rc^*}]$ ($n=2$ and 3) were newly isolated, but $[\mathrm{Rc^*(C{\equiv}C)_4Rc^*}]$ could generate no stable oxidized species. The dications of $[\mathrm{Rc^*(C{\equiv}C)_{\mathit{n}}Rc^*}]$ ($n=1$–3) were unstable in solution and produced a bis(fulvene)-type complex, which is probably due to the generation of a biradical on the bridging chain. The stability of the two-electron-oxidized species of $[\mathrm{Rc^*(C{\equiv}C)_{\mathit{n}}Rc^*}]$ tends to decrease with the increase in the number of C≡C units. This suggests that the spin coupling, which causes the structural isomerization to a fulvene complex, is weakened with the elongation of the bridging C≡C chain.

Experimental Section

All reactions were carried out under an atmosphere of N_2 and/or Ar and workups were performed without precautions to exclude air. NMR spectra were recorded on Bruker AC300P, AM400 or ARX400 spectrometers. IR (KBr disc) spectra were recorded on Perkin–Elmer System 2000 spectrometer. Cyclic voltammetry was carried out by using BAS ALS600 in 10^{-1} M solution of $n\mathrm{Bu_4NClO_4}$ (polarography grade, Nacalai tesque) in $\mathrm{CH_2Cl_2}$. CV cells were fitted with glassy carbon (GC) working electrode, Pt wire counter electrode and $\mathrm{Ag/Ag^+}$ pseudoreference electrode. The cyclic voltammograms were obtained at a scan rate of $0.1\ \mathrm{Vs^{-1}}$ on the 5×10^{-4} M solutions of the complexes. All potentials were referenced vs $\mathrm{FcH/FcH^+}$ and were obtained by the preceding measurement of ferrocene at the same conditions (0.22 V for Ag/Ag+). Thin-layer coulometry was carried out on apparatus described previously.[39] Dry solvents were prepared by distillation from a drying agent prior to use as follows: $\mathrm{CH_2Cl_2}$ ($\mathrm{CaCl_2}$); benzene (Na); toluene (Na); pyridine (KOH); THF (Na-benzophenone); ether ($\mathrm{LiAlH_4}$). 1-(1″,2″,3″,4″,5″-Pentamethylruthenocenyl)ethyne,[40] 1-(2′,3′,4′,5′-tetramethylruthenocenyl)ethyne,[41] 1-(1″,2″,3″,4″,5″-pentamethylruthenocenyl)propyne (**2**),[28] and 1-(2′,3′,4′,5′-tetra-methylruthenocenyl) propyne (**3**)[28] were prepared according to literature procedures. Other reagents were used as received from commercial suppliers.

Bis(1″,2″,3″,4″,5″-pentamethylruthenocenyl)ethyne (5):[28] A solution of **2** (0.34 g, 1 mmol), $[\mathrm{Mo(CO)_6}]$ (52 mg, 0.2 mmol), and $2\text{-}\mathrm{FC_6H_4OH}$ (0.11 g, 1 mmol) in toluene (4 mL) was refluxed under bubbling of Ar for 2 h. After cooling to room temperature, the solution was quenched with 0.5% aqueous NaOH (20 mL) and the mixture was extracted with diethyl ether. The organic extract was washed with the 0.5% aqueous NaOH and then water. After drying over $\mathrm{MgSO_4}$, the solution was evaporated. The residue was subject to chromatography on $\mathrm{SiO_2}$ by elution of hexane to give the recovered starting material (20 mg, 6%) and **5** (189 mg, 60%) as pale yellow crystals.

Bis(2′,3′,4′,5′-tetramethylruthenocenyl)ethyne (6): This complex was prepared from **3** according to the procedure described above. Pale yellow crystals (22%). M.p. 188–189 °C; elemental analysis calcd (%) for $\mathrm{C_{30}H_{34}Ru_2}$: C 60.38, H 5.74; found: C 60.54, H 5.69; UV/Vis ($\mathrm{CH_2Cl_2}$): $\lambda_{\max}$ (ε) = 232 (26500), 279 (14200), 328 nm ($3100\ \mathrm{mol^{-1}dm^3cm^{-1}}$); ^{1}H NMR (400 MHz, $\mathrm{CDCl_3}$, TMS): δ = 1.97 (s, 12H; Me), 2.08 (s, 12H; Me), 4.25 ppm (s, 10H; $\eta\text{-}\mathrm{C_5H_5}$); ^{13}C NMR (100 MHz , $\mathrm{CDCl_3}$, TMS): δ = 12.32 (Me), 12.99 (Me), 71.26 (C), 73.12 ($\eta\text{-}\mathrm{C_5H_5}$), 85.82 ($\eta\text{-}\mathrm{C_5Me_4}$-ipso), 86.08 ($\eta\text{-}\mathrm{C_5Me_4}$), 86.63 ppm ($\eta\text{-}\mathrm{C_5Me_4}$).

(*E*)-[Rc′(*p*-ClC$_6$H$_4$O)C=CH(Me)] (7): When a solution of **3** (0.32 g, 1 mmol), $[\mathrm{Mo(CO)_6}]$ (26 mg, 0.1 mmol), and $4\text{-}\mathrm{ClC_6H_4OH}$ (0.13 g, 1 mmol) in toluene (4 mL) was allowed to react under similar conditions to those described above for the preparation of compound **5**, complex **7** (0.34 g, 76%) was obtained as the main product and the alkyne derivative **6** was detected in trace yield by the ^{1}H NMR spectrum. Data for **7**: Colorless solid; M.p. 80–82 °C; elemental analysis calculated (%) for $\mathrm{C_{23}H_{25}ClORu}$: C 60.85, H 5.55; found: C 61.23, H 5.65; ^{1}H NMR (400 MHz, $\mathrm{CDCl_3}$, TMS): δ = 1.66 (brs, 3H; Me), 1.96 (s, 6H; Me), 1.98 (s, 6H; Me), 4.13 (s, 5H; $\eta\text{-}\mathrm{C_5H_5}$), 5.26 (q, ^3J(H,H) = 7.2 Hz, 1H; =CH), 6.92 (brd, ^3J(H,H) = 7.6 Hz, 2H; $\mathrm{C_6H_4}$), 7.23 ppm (d, ^3J(H,H) = 8.7 Hz, 2H; $\mathrm{C_6H_4}$); ^{13}C NMR (100 MHz, $\mathrm{CDCl_3}$, TMS): δ = 12.31 (Me), 13.12 (Me), 72.98 ($\eta\text{-}\mathrm{C_5H_5}$), 85.00 ($\eta\text{-}\mathrm{C_5Me_4}$), 86.01 ($\eta\text{-}\mathrm{C_5Me_4}$), 111.48 ($\mathrm{C_6H_4}$), 119.03 ($\mathrm{C_6H_4}$), 126.47 ($\mathrm{ClC_6H_4}$), 129.10 (=C−H), 149.34 (=C−O), 156.15 ppm ($\mathrm{OC_6H_4}$).

1,4-Bis(1″,2″,3″,4″,5″-pentamethylruthenocenyl)-1,3-butadiyne (9): A solution of 1-(1″,2″,3″,4″,5″-pentamethylruthenocenyl)ethyne (325 mg, 1.0 mmol) in pyridine (25 mL) was added to a solution of CuCl (99 mg, 1 mmol), DBU (304 mg, 2 mmol) in pyridine (5 mL). The mixture was stirred for 3.5 h under bubbling of O_2 at 50 °C. The reaction mixture was diluted with benzene (20 mL). The mixture was washed with dilute aqueous HCl and then water. After drying over $\mathrm{MgSO_4}$ and then evaporating under reduced pressure, the residue was subjected to chromatography on $\mathrm{Al_2O_3}$ (deactivated with 5% $\mathrm{H_2O}$) by elution with benzene. The crystals obtained were recrystallized from cyclohexane/hexane to give **9**. Pale yellow fine crystals (77%); m.p. 230 °C (decomp); elemental analysis calcd (%) for $\mathrm{C_{34}H_{38}Ru_2}$: C 62.94, H 5.90; found: C 63.25, H 6.03; IR (KBr): $\tilde{\nu}$ = 2219, 2150 cm^{-1} (C≡C); UV/Vis ($\mathrm{CH_2Cl_2}$): λmax (ε) = 230 (32800), 274 (20600), 309 (13900), 341 nm ($10500\ \mathrm{mol^{-1}dm^3cm^{-1}}$); ^{1}H NMR (400 MHz, $\mathrm{CDCl_3}$, TMS): δ = 1.89 (s, 30H; Me), 4.23 (t, ^3J(H,H) = 1.7 Hz, 4H; $\eta\text{-}\mathrm{C_5H_4}$), 4.40 ppm (t, ^3J(H,H) = 1.7 Hz, 4H; $\eta\text{-}\mathrm{C_5H_4}$); ^{13}C NMR (100 MHz, $\mathrm{CDCl_3}$, TMS): δ = 11.40 (Me), 65.27 (≡C), 70.81 (≡C), 73.47 ($\eta\text{-}\mathrm{C_5H_4}$), 77.25 ($\eta\text{-}\mathrm{C_5H_4}$), 77.54 (ipso-$\eta\text{-}\mathrm{C_5H_4}$), 85.96 ppm ($\eta\text{-}\mathrm{C_5Me_5}$).

1,4-Bis(2′,3′,4′,5′-tetramethylruthenocenyl)buta-1,3-diyne (10):[41] This compound was also prepared in 72% yield from 1-(2′,3′,4′,5′-tetramethylruthenocenyl)ethyne according to the procedure described for the preparation of **9**.

3-(1″,2″,3″,4″,5″-Pentamethylruthenocenyl)propyn-1-al (13): A 1.6 M solution of nBuLi in hexane (1.1 mL, 1.6 mmol) was added to a solution of 1-(1″,2″,3″,4″,5″-pentamethylruthenocenyl)ethyne (0.48 g, 1.5 mmol) in absolute THF (10 mL) below −78 °C under Ar. After the solution had been stirred at this temperature for 30 min, DMF (0.15 mL, 1.8 mmol) was added slowly. The solution was warmed gradually to room temperature over a period of 1.5 h and then quenched with saturated aqueous $\mathrm{NH_4Cl}$ (40 mL). The mixture was extracted with diethyl ether (40 mL) and then the ether extract was washed with $\mathrm{H_2O}$ (40 mL × 3). The ether phase was dried over $\mathrm{MgSO_4}$ and then evaporated in vacuo. The residue was subjected to chromatography on $\mathrm{SiO_2}$ by elution with benzene to give compound **13**. Orange crystals (95 %); M.p. 93–94 °C; elemental analysis calcd (%) for $C_{18}H_{20}ORu$: C 61.17, H 5.70; found: C 61.21, H, 5.66; IR (KBr): $\tilde{\nu}=2167$ (C≡C), 1652 cm^{-1} (CO); ^1H NMR (400 MHz, $CDCl_3$, TMS): $\delta=1.87$ (s, 15 H; Me), 4.41 (t, $^3J(H,H)=1.7$ Hz, 2 H; η-C_5H_4), 4.50 (t, $^3J(H,H)=1.7$ Hz, 2 H; η-C_5H_4), 9.33 ppm (s, 1 H; CHO); ^{13}C NMR (100 MHz, $CDCl_3$, TMS): $\delta=11.30$ (Me), 63.00 (≡C), 75.69 (η-C_5H_4), 76.74 (η-C_5H_4), 86.67 (η-C_5Me_5), 88.80 (ipso-η-C_5H_4), 99.93 (≡C), 176.47 ppm (CO).

1-(1″,2″,3″,4″,5″-Pentamethylruthenocenyl)-4-trimethylsilyl-1,3-butadiyne (14): A 2.0 M solution of Me_3SiCHN_2 in hexane (1.0 mL, 1.8 mmol) was slowly added to a solution of LDA prepared from $(i\text{Pr})_2NH$ (0.3 mL, 2.0 mmol) and a 1.6 M solution of *n*BuLi in hexane (1.1 mL, 1.8 mmol) in dry THF (15 mL) below −78 °C. After the solution had been stirred for 30 min at this temperature, a solution of **13** (0.54 g, 1.5 mmol) in dry THF (5 mL) was added dropwise. The solution was stirred for a further 1 h at this temperature and then gradually warmed to room temperature. After stirring for 4 h at room temperature, the solution was again cooled below −78 °C and a 1.6 M solution of *n*BuLi in hexane (1.1 mL, 1.8 mmol) was added. The solution was slowly warmed to room temperature and then quenched with saturated aqueous $NaHCO_3$ (40 mL). The mixture was extracted with diethyl ether (40 mL) and then the ether extract was washed with H_2O (40 mL × 4). The ether phase was dried over $MgSO_4$ and then evaporated in vacuo. The residue was subjected to chromatography on Al_2O_3 (deactivated with 5 % H_2O) by elution with pentane to give compound **14**. This compound was thermally unstable and changed color to brown in air. Fine yellow crystals (95 %); MS (70 eV): *m*/*z* (%): 422 (100) [M^+]; ^1H NMR (400 MHz, $CDCl_3$, TMS): $\delta=0.21$ (s, 9 H; Me), 1.89 (s, 15 H; Me), 4.23 (t, $^3J(H,H)=1.7$ Hz, 2 H; η-C_5H_4), 4.38 ppm (t, $^3J(H,H)=1.7$ Hz, 2 H; η-C_5H_4); ^{13}C NMR (100 MHz, $CDCl_3$, TMS): δ −0.25 (Me), 11.16 (Me), 66.01 (≡C), 70.40 (≡C), 73.74 (η-C_5H_4), 76.37 (η-C_5H_4), 76.50 (ipso-η-C_5H_4), 86.19 (η-C_5Me_5), 87.19 (≡C), 89.98 ppm (≡C).

1-(1″,2″,3″,4″,5″-pentamethylruthenocenyl)-1,3-butadiyne (15): KOH in methanol (1 M, 2 mL) was added to a solution of **14** (0.34 g, 0.87 mmol) in dry diethyl ether (5 mL). After stirring for 2 h, the solution was quenched with saturated aqueous NH_4Cl (20 mL). The mixture was extracted with diethyl ether (20 mL) and then the ether extract was washed with H_2O (10 mL × 3). The ether phase was dried over $MgSO_4$ and then evaporated in vacuo. The residue was subjected to chromatography on SiO_2 by elution of pentane containing diethyl ether (2.5 %) to give compound **15**. This compound changed color to brown in air. Yellow crystals (98 %); MS (70 eV): *m*/*z* (%): 349 (100) [M^+]; ^1H NMR (400 MHz, $CDCl_3$, TMS): $\delta=1.89$ (s, 15 H; Me), 2.35 (s, 1 H), 4.25 (t, $^3J(H,H)=1.7$ Hz, 2 H; η-C_5H_4), 4.41 ppm (t, $^3J(H,H)=1.7$ Hz, 2 H; η-C_5H_4).

1-Iodo-2-(1″,2″,3″,4″,5″-pentamethylruthenocenyl)ethyne (16): A 1.6 M solution of *n*BuLi in hexane (0.9 mL, 1.3 mmol) was added to a solution of [Rc*C≡CH] (0.38 g, 1.2 mmol) in absolute THF (15 mL) below −78 °C under Ar. After stirring for 30 min at this temperature, iodine (0.31 g, 1.2 mmol) was added quickly to the solution. The mixture was stirred for a further 30 min and then gradually warmed to room temperature. The resulting violet solution was quenched with saturated aqueous NH_4Cl (40 mL). The mixture was extracted with diethyl ether (40 mL). The ether extract was washed with saturated aqueous $Na_2S_2O_3$ (three times) and water, and then dried over $MgSO_4$. After evaporating in vacuo, the residue was subjected to chromatography on Al_2O_3 (deactivated with 5 % H_2O) by elution of pentane containing diethyl ether. Greenish-yellow crystals (0.39 g, 72 %); MS (70 eV): *m*/*z* (%): 452 (80) [M^+], 325 (100); ^1H NMR (400 MHz, $CDCl_3$, TMS): $\delta=1.90$ (s, 15 H; Me), 4.26 (t, $^3J(H,H)=1.8$ Hz, 2 H; η-C_5H_4), 4.42 ppm (t, $^3J(H,H)=1.8$ Hz, 2 H; η-C_5H_4); ^{13}C NMR (100 MHz, C_6D_6, TMS): $\delta=11.15$ (Me), 65.90 (≡C), 72.39 (≡C), 74.03 (η-C_5H_4), 76.91 (η-C_5H_4), 79.86 (ipso-η-C_5H_4), 86.19 ppm (η-C_5Me_5).

1,6-Bis(1″,2″,3″,4″,5″-pentamethylruthenocenyl)hexa-1,3,5-triyne (11): A mixture of **15** (87 mg, 0.25 mmol), **16** (58 mg, 0.13 mmol), and CuI (10 mg, 0.05 mmol) in pyrrolidine (0.5 mL) was stirred at room temperature for 30 min under nitrogen. To the resulting red-orange solution was added saturated aqueous NH_4Cl (10 mL). The mixture was extracted with diethyl ether (50 mL). The ether extract was washed with 0.5 % aqueous H_2SO_4 solution (10 mL × 2) and H_2O (20 mL), and then dried over $MgSO_4$. After evaporation in vacuo, the residue was subjected to chromatography on silica gel by elution of hexane containing diethyl ether (5 %) to give compound **11**. Orange-yellow crystals (72 %); m.p. 239 °C; elemental analysis calcd (%) $C_{36}H_{38}Ru_2$: C 64.26, H 5.69; found: C 64.25, H 5.62; MS (70 eV): *m*/*z* (%):674 (20) [M^+], 649 (100); IR (KBr): $\tilde{\nu}=2196$ cm^{-1} (C≡C); UV/Vis (CH_2Cl_2): λ_{max} (ε) = 234 (56100), 300 (22600), 360 (10000), 390 nm (9600 $mol^{-1}dm^3cm^{-1}$); ^1H NMR (400 MHz, $CDCl_3$, TMS): $\delta=1.89$ (s, 30 H; Me), 4.26 (t, $^3J(H,H)=1.7$ Hz, 4 H; η-C_5H_4), 4.42 ppm (t, $^3J(H,H)=1.7$ Hz, 4 H; η-C_5H_4); ^{13}C NMR (100 MHz, $CDCl_3$, TMS): δ 11.39 (Me), 65.15 (≡C), 65.93 (≡C), 71.24 (≡C), 73.96 (η-C_5H_4), 76.55 (η-C_5H_4), 77.50 (ipso-η-C_5H_4), 86.30 ppm (η-C_5Me_5).

1,8-Bis(1″,2″,3″,4″,5″-pentamethylruthenocenyl)octa-1,3,5,7-tetrayne (12): A mixture of **15** (0.30 g, 0.85 mmol) and CuI (0.5 g, 2.6 mmol) in pyridine (20 mL) was stirred at room temperature overnight under bubbling of air. The mixture was diluted with Et_2O (40 mL) and then filtered under reduced pressure. The precipitate was washed with Et_2O and the filtrate and washing were combined. The organic layer was washed three times with 1 % aqueous H_2SO_4 solution (50 mL) and with H_2O (20 mL), and then dried over $MgSO_4$. After evaporation in vacuo, the residue was subjected to chromatography on silica gel by elution of hexane containing benzene (10 %) to give compound **12**. Yellow crystals (70 %); m.p. 231 °C (decomp); elemental analysis calcd (%) for $C_{38}H_{38}Ru_2$: C 65.50, H 5.50; found: C 65.58, H 5.45; MS (70 eV): *m*/*z* (%): 697 (100) [M^+]; IR (KBr): $\tilde{\nu}=2192$ cm^{-1} (C≡C); UV/Vis (CH_2Cl_2): λ_{max} (ε) = 226 (71200), 250 (52400), 301 (30800), 318 (27100), 368 (13800), 397 (14900), 432 nm (11000 $mol^{-1}dm^3cm^{-1}$); ^1H NMR (400 MHz, C_6D_6, TMS): $\delta=1.88$ (s, 30 H; Me), 4.11 (t, $^3J(H,H)=1.7$ Hz, 4 H; η-C_5H_4), 4.43 ppm (t, $^3J(H,H)=1.7$ Hz, 4 H; η-C_5H_4); ^{13}C NMR (100 MHz, C_6D_6, TMS): $\delta=10.85$ (Me), 64.62 (≡C), 65.09 (≡C), 65.98 (≡C), 71.61 (≡C), 73.91 (η-C_5H_4), 76.56 (η-C_5H_4), 77.98 (ipso-η-C_5H_4), 85.97 ppm (η-C_5Me_5).

[Ru_2(μ_2-η^6:η^6-$C_5Me_4C{=}CC_5Me_4$)(η-C_5H_5)$_2$](BF_4)$_2$ (19): One drop of $BF_3{\cdot}OEt_2$ was added to a solution of **6** (18 mg, 0.03 mmol) and *p*-BQ (6.3 mg, 0.06 mmol) in CH_2Cl_2 (4 mL) at 0 °C under nitrogen. Immediately, the solution changed color from yellow to deep red and an amorphous precipitate formed. The mixture was stirred for 4 h and then the precipitate was collected by filtration, giving a yellow powder (80 %). Recrystallization from CH_3NO_2/Et_2O produced orange crystals. M.p. > 250 °C; elemental analysis calcd (%) for $C_{30}H_{34}B_2F_8Ru_2$: C 46.77, H 4.45; found: C 46.35, H 4.22; ^1H NMR (400 MHz, CD_3NO_2, TMS): $\delta=2.04$ (s, 12 H; Me), 2.32 (s, 12 H; Me), 5.40 ppm (s, 10 H; η-C_5H_5); ^{13}C NMR (100 MHz, CD_3NO_2, TMS): $\delta=11.82$ (Me), 78.67 (=C=), 91.60 (η-C_5H_5), 102.32 (η-C_5Me_4), 112.71 (η-C_5Me_4), 141.86 ppm (ipso-η-C_5Me_4).

[Ru_2(μ_2-η^6:η^6-$C_5H_4C{=}C{=}C{=}CC_5H_4$)(η-$C_5Me_5$)$_2$]($BF_4$)$_2$ (20): One drop of $BF_3{\cdot}OEt_2$ was added to a solution of **9** (19.5 mg, 0.03 mmol) and *p*-BQ (6.3 mg, 0.06 mmol) in CH_2Cl_2 (4 mL) and benzene (2 mL) at 0 °C under nitrogen. Immediately, the solution changed color from yellow to red-brown. The mixture was kept for 2 h at 0 °C. The resulting precipitate was collected by filtration and washed with a small amount of dry diethyl ether, giving yellow-brown powder (80 %). ^1H NMR (400 MHz, CD_3NO_2, −20 °C): $\delta=2.05$ (s, 30 H; Me), 5.24 (t, $^3J(H,H)=1.8$ Hz, 4 H; η-C_5H_4), 6.22 ppm (t, $^3J(H,H)=1.8$ Hz, 4 H; η-C_5H_4); ^{13}C NMR (100 MHz, CD_3NO_2, −20 °C): $\delta=8.04$ (Me), 78.54 (=C=), 81.59 (η-C_5H_4), 97.02 (η-C_5H_4), 101.48 (η-C_5Me_5), 136.80 (ipso-η-C_5H_4), and 148.66 (=C=). Complex **20** was unstable even at 0 °C. Besides the signals of **20**, new signals for **24** was also observed: ^1H NMR (400 MHz, CD_3NO_2, 0 °C): $\delta=2.24$ (s, 30 H; Me), 5.02 (t, $^3J(H,H)=2.0$ Hz, 2 H; η-C_5H_4), 5.41 (t, $^3J(H,H)=2.0$ Hz, 2 H; η-C_5H_4), 5.57 (t, $^3J(H,H)=2.0$ Hz, 2 H; η-C_5H_4), 6.17 (t, $^3J(H,H)=2.0$ Hz, 2 H; η-C_5H_4), 6.68 ppm (s, 2 H; =CH); ^{13}C NMR (100 MHz, CD_3NO_2, 0 C): $\delta=9.84$ (Me), 70.26 (C), 81.73 (η-C_5H_4), 84.22 (η-C_5H_4), 86.48 (=CH), 96.42 (η-C_5H_4), 98.41 (η-C_5H_4), 102.46 ppm (η-C_5Me_5).

MO calculations: DFT calculations were performed with Gaussian 98 program[42] running on the workstations assembled by HIT Inc. The ynediyl-, diynediyl-, and triynediyl-bridged binuclear ruthenocenes and their two-electron-oxidized species were optimized fully by using a standard 3–21G(d) basis set and B3LYP functional, which incorporated the three-parameter exchange functional by Becke[43] with the correlation functional by Lee, Yang, and Parr[44] (B3LYP/3–21G(d)). Molecular orbital energy levels, together with the orbital diagrams were obtained from B3LYP/3–21G(d) calculations. The graphic representations of the calculated molecular orbitals were obtained using GaussView.[45]

Structure determination: The crystallographic data are listed in Table 1 for **7** and **19**. Data collection of crystal data for **7** and **19** were performed at room temperature on a Mac Science DIP3000 image processor and a Bruker Apex diffractometer with graphite-monochromated $Mo_{K\alpha}$ radiation and an 18 kW rotating anode generator, respectively. The structure of **7** was solved with the Dirdif-Patty method in MAXUS (software-package for structure determination) and refined finally by full-matrix least-squares procedure with SHELXL.[46] The structure of **19** was solved and refined by SHELXL.[46] The absorption correction for **7** was carried out by the Sortav method and anisotropic refinement for non-hydrogen atom was also performed. The hydrogen atoms, located from difference Fourier maps or calculation, were isotropically refined.

CCDC–279678 (**7**) and CCDC-279679 (**19**) contain the supplementary crystallographic data for this paper. These data can be obtained free of charge from The Cambridge Crystallographic Data Centre via www.ccdc.cam.ac.uk/data_request/cif.

Acknowledgements

The present work was supported by Grant-in-Aid for Science Research (No. 10640538) from the Ministry of Education, Science, and Culture of Japan.

[1] a) W. Beck, B. Niemer, M. Wieser, *Angew. Chem.* **1993**, *105*, 969; *Angew. Chem. Int. Ed. Engl.* **1993**, *32*, 923; b) H. Lang, *Angew. Chem.* **1994**, *106*, 569; *Angew. Chem. Int. Ed. Engl.* **1994**, *33*, 547; c) A. Nakamura, *Bull. Chem. Soc. Jpn.* **1995**, *68*, 1515; d) N. J. Long, *Angew. Chem.* **1995**, *107*, 37; *Angew. Chem. Int. Ed. Engl.* **1995**, *34*, 21; e) U. H. F. Bunz, *Angew. Chem.* **1996**, *108*, 1047; *Angew. Chem. Int. Ed. Engl.* **1996**, *35*, 969.

[2] D. Astruc, *Electron Transfer and Radical Process in Transition-metal Chemistry*, VCH, New York, **1995**.

[3] *Mixed-Valence Compounds*, (Ed.: D. H. Brown), Reidel, Dordrecht, **1980**.

[4] A. Togni, T. Hayashi, *Ferrocenes*, VCH, New York, **1995**.

[5] a) A. Wong, P. C. W. Kang, C. D. Tagge, D. R. Leon, *Organometallics* **1990**, *9*, 1992; b) R. Crescenzi, C. L. Sterzo, *Organometallics* **1992**, *11*, 4301.

[6] a) J. W. Seyler, W. Weng, Y. Zhou, J. A. Gladysz, *Organometallics* **1993**, *12*, 3802; b) Y. Zhou, J. W. Seyler, W. Weng, A. M. Arif, J. A. Gladysz, *J. Am. Chem. Soc.* **1993**, *115*, 8509; c) M. Brady, W. Weng, Y. Zhou, J. W. Seyler, A. J. Amoroso, A. M. Arif, M. Böhme, G. Frenking, J. A. Gladysz, *J. Am. Chem. Soc.* **1997**, *119*, 775; d) M. Brady, W. Weng, J. A. Gladysz, *J. Chem. Soc. Chem. Commun.* **1994**, 2655; e) T. Bartik, B. Bartik, M. Brady, R. Dembinski, J. A. Gladysz, *Angew. Chem.* **1996**, *108*, 467; *Angew. Chem. Int. Ed. Engl.* **1996**, *35*, 414; f) R. Dembinski, T. Bartik, B. Bartik, M. Jaeger, J. A. Gladysz, *J. Am. Chem. Soc.* **2000**, *122*, 810; g) R. C. Horn, J. M. Martín-Alvarez, J. A. Gladysz, *Organometallics* **2002**, *21*, 5386; h) R. C. Horn, J. A. Gladysz, *Eur. J. Inorg. Chem.* **2003**, 2211.

[7] a) N. Le Narvor, C. Lapinte, *J. Chem. Soc. Chem. Commun.* **1993**, 357; b) N. Le Narvor, L. Toupet, C. Lapinte, *J. Am. Chem. Soc.* **1995**, *117*, 7129; c) F. Coat, C. Lapinte, *Organometallics* **1996**, *15*, 477; d) F. Coat, M.-A. Guillevic, L. Toupet, F. Paul, C. Lapinte, *Organometallics* **1997**, *16*, 5988; e) M. Guillemot, L. Toupet, C. Lapinte, *Organometallics* **1998**, *17*, 1928; f) F. Paul, C. Lapinte, *Coord. Chem. Rev.* **1998**, *178*/180, 431; g) F. Paul, W. E. Meyer, L. Toupet, H. Jiano, J. A. Gladysz, C. Lapinte, *J. Am. Chem. Soc.* **2000**, *122*, 9405; h) F. Coat, F. Paul, L. Loupet, K. Costuas, J.-F. Halet, *J. Organomet. Chem.* **2003**, *683*, 368; i) H. Jiano, K. Costuas, J. A. Gladysz, J.-F. Halet, M. Guillemot, L. Toupet, F. Paul, C, Lapinte, *J. Am. Chem. Soc.* **2003**, *125*, 9511.

[8] a) M. Akita, M.-C. Chung, A. Sakurai, S. Sugimoto, M. Terada, M. Tanaka, Y. Moro-oka, *Organometallics* **1997**, *16*, 4882; b) M. Akita, A. Sakurai, M.-C. Chung, Y. Moro-oka, *J. Organomet. Chem.* **2003**, *670*, 2.

[9] a) M. I. Bruce, P. Hinterding, E. R. Tiekink, *J. Organomet. Chem.* **1993**, *450*, 209; b) M. I. Bruce, L. I. Denisovich, P. L. Low, S. M. Peregudova, N. A. Vstynyuk, *Mendeleev Commun.* **1996**, 200; c) M. I. Bruce, B. D. Kelley, B. W. Skelton, A. H. White, *J. Organomet. Chem.* **2000**, *604*, 150; d) M. I. Bruce, P. J. Low, K. Costuas, J.-F. Halet, S. P. Best, G. A. Heath, *J. Am. Chem. Soc.* **2000**, *122*, 1949; e) M. I. Bruce, B. G. Ellis, P. L. Low, B. W. Skelton, A. H. White, *Organometallics* **2003**, *22*, 3184.

[10] S. Rigant, J. Rerruchon, L. L. Pichon, D. Touchard, P. H. Dixneuf, *J. Organomet. Chem.* **2003**, *670*, 37.

[11] a) Y.-L. Yang, J.-J. Wang, Y.-C. Lin, S.-L. Huang, M.-C. Chen, G.-H. Lee, Y. Wang, *Organometallics* **1997**, *16*, 1573; b) M. I. Bruce, M. Ke, P. J. Low, *Chem. Commun.* **1996**, 2405.

[12] U. H. F. Bunz, V. Enkelman, F. Beer, *Organometallics* **1995**, *14*, 2490.

[13] a) S. Kheradmandan, K. Heinze, H. W. Schmalle, H. Berke, *Angew. Chem.* **1999**, *111*, 2412; *Angew. Chem. Int. Ed.* **1999**, *38*, 2270; b) F. J. Fernández, K. Venkatesan, O. Blacque, H. W. Schmalle, H. Berke, *Chem. Eur. J.* **2003**, *9*, 6192; c) S. Kheradmandan, K. Venkatesan, O. Blacque, H. W. Schmalle, H. Berke, *Chem. Eur. J.* **2004**, *10*, 4872.

[14] a) W. Mohr, J. Stahl, F. Hampel, J. A. Gladysz, *Inorg. Chem.* **2001**, *40*, 3263; b) J. Stahl, J. C. Bohling, E. B. Bauer, T. B. Peters, W. Mohr, J. M. Martín-Alvarez, F. Hampel, J. A. Gladysz, *Angew. Chem.* **2002**, *114*, 1951; *Angew. Chem. Int. Ed.* **2002**, *41*, 1872; c) W. Mohr, J. Stahl, F. Hampel, J. A. Gladysz, *Chem. Eur. J.* **2003**, *9*, 3324; d) W. Mohr, J. Stahl, F. Hampel, J. A. Gladysz, *Organometallics* **2004**, *23*, 5889.

[15] a) V. W.-W. Yam, K. M.-C. Wong, N. Zhu, *Angew. Chem.* **2003**, *115*, 1438; *Angew. Chem. Int. Ed.* **2003**, *42*, 1400; b) C. Muller, R. J. Lachicotte, W. D. Jones, *Organometallics* **2002**, *21*, 1190.

[16] a) C. M. Che, H. Y. Chao, V. M. Miskowski, Y. Li, K. K. Cheung, *J. Am. Chem. Soc.* **2001**, *123*, 4985; b) W. Lu, H. F. Xiang, N. Zhu, C. M. Che, *Organometallics* **2002**, *21*, 2343.

[17] C. Elschenbroich, J. Plackmeyer, M. Nowotny, K. Harms, J. Pebler, O. Burghaus, *Inorg. Chem.* **2005**, *44*, 955.

[18] a) G. H. Worth, B. H. Robinson, J. Simpson, *Organometallics* **1992**, *11*, 501; b) G. H. Worth, B. H. Robinson, J. Simpson, *Organometallics* **1992**, *11*, 3863.

[19] a) M. Altman, V. Enkelman, F. Beer, U. H. F. Bunz, *Organometallics* **1996**, *15*, 394; b) M. Altman, V. Enkelman, F. Beer, U. H. F. Bunz, *Chem. Ber.* **1996** *129*, 269; c) J. Classen, R. Gleiter, F. Rominger, *Eur. J. Inorg. Chem.* **2002**, 2040.

[20] a) H. Yao, M. Sabat, R. N. Grimes, P Zanello, F. Fabrizi de Biani, *Organometallics* **2003**, *22*, 2581; b) F. Fabrizi de Biani, M. Corsini, P. Zanello, H. Yao, R. N. Grimes, *J. Am. Chem. Soc.* **2004**, *126*, 11360.

[21] a) Y. Kasahara, Y. Hoshin, M. Kajitani, K. Simizu, G. R. Sato, *Organometallics* **1992**, *11*, 1968; b) Y. Hoshin, S. Higuchi, J. Fiedler, C.-Y. Su, A. Knödler, B. Schwederski, B. Sarkar, H. Hartmann, W. Kaim, *Angew. Chem.* **2003**, *115*, 698; *Angew. Chem. Int. Ed.* **2003**, *42*, 674.

[22] a) S. N. Miligan, R. D. Rieke, *Organometallics* **1983**, *2*, 171; b) R. D. Rieke, S. N. Miligan, L. D. Schulte, *Organometallics* **1987**, *6*, 699.

[23] a) N. G. Connelly, A. R. Lucy, J. D. Payne, A. M. R. Galas, W. E. Geiger, *J. Chem. Soc. Dalton Trans.* **1983**, 1879; b) M. J. Freeman, A. G. Orpen, N. G. Connery, I. Manners, S. J. Raven, *J. Chem. Soc. Dalton Trans.* **1985**, 2283.

[24] a) J. Edwin, W. E. Geiger, *J. Am. Chem. Soc.* **1990**, *112*, 7104; b) W. E. Geiger, A. Salzer, J, Edwin, W. Vonpilipsborn, U. Paiantini, A. L. Rheigold, *J. Am. Chem. Soc.* **1990**, *112*, 7121.

[25] a) M. Lacoste, L. Varret, L. Toupet, D. Astruc, *J. Am. Chem. Soc.* **1987**, *109*, 6504; b) D. Astruc, M. Lacoste, L. Toupet, *J. Chem. Soc. Chem. Commun.* **1990**, 558; c) M. Lacoste, H. Rabaa, D. Astruc, M. Ardoin, F. Varret, J.-Y. Saillard, A. LeBeuze, *J. Am. Chem. Soc.* **1990**, *112*, 9548; d) M.-H. Delville, M. Lacoste, D. Astruc, *J. Am. Chem. Soc.* **1992**, *114*, 8310.

[26] M. Watanabe, M. Sato, *Organometallics* **1999**, *18*, 5201.
[27] a) M. Sato, Y. Kawata, A. Kudo, A. Iwai, H. Saitoh, S. Ochiai, *J. Chem. Soc. Dalton Trans.* **1998**, 2215; b) M. Sato, A. Kudo, Y. Kawata, H. Saitoh, *Chem. Commun.* **1996**, 25.
[28] M. Sato, M. Watanabe, *Chem. Commun.* **2002**, 1574.
[29] A.-C. Ribou, J.-P. Launoy, H. L. Sachtleben, C. W. Spangler, *Inorg. Chem.* **1996**, *35*, 3735.
[30] W. Skibar, H. Kopacka, K. Wurst, C. Salzmann, K.-H. Ongania, F. Fabrizi de Biani, P. Zanello, B. Bildstein, *Organometallics* **2004**, *23*, 1024.
[31] M.; Sato, T. Nagata, T. Fujihara, S. Kumakura, K. Unoura, *Chem. Eur. J.* **2004**, *10*, 2166.
[32] a) A. Mortreux, M. Blanchard, *J. Chem. Soc. Chem. Commun.* **1974**, 786; b) N. Kaneta, T Hirai, M. Mori, *Chem. Lett.* **1995**, 627; c) N. G. Pschirer, U. F. Bunz, *Tetrahedron Lett.* **1999**, *40*, 2481.
[33] K. Grela, J. Ignatowska, *Org. Lett.* **2002**, *4*, 3747.
[34] O. Hofer, K. Schlögl, *J. Organomet. Chem.* **1968**, *13*, 443.
[35] F. Zhuravlev, J. A. Gladysz, *Chem. Eur. J.* **2004**, *10*, 6510.
[36] S. Barlow, A. Cowley, J. C. Green, T. J. Brunker, T. Hascall, *Organometallics* **2001**, *20*, 5351.
[37] A. I. Yanovsky, Y. T. Struchkov, M. I. Rybinskaya, *J. Organomet. Chem.* **1989**, *369*, 125.
[38] J. P. C. M. van Dongen, M. J. A. de Bie, R. Steur, *Tetrahedron Lett.* **1973**, *14*, 1371.
[39] K. Unoura, A. Iwase, H. Ogino, *J. Electroanal. Chem. Interfacial Electrochem.* **1990**, *295*, 385.
[40] M. Sato, Y. Kawata, H. Shintate, Y. Habata, S. Akabori, K. Unoura, *Organometallics* **1997**, *16*, 1693.
[41] M. Sato, A. Iwai, M. Watanabe, *Organometallics* **1999**, *18*, 3208.
[42] Gaussian 98, Revision A.11.3, M. J. Frisch, G. W. Trucks, H. B. Schlegel, G. E. Scuseria, M. A. Robb, J. R. Cheeseman, V. G. Zakrzewski, J. A. Montgomery, Jr., R. E. Stratmann, J. C. Burant, S. Dapprich, J. M. Millam, A. D. Daniels, K. N. Kudin, M. C. Strain, O. Farkas, J. Tomasi, V. Barone, M. Cossi, R. Cammi, B. Mennucci, C. Pomelli, C. Adamo, S. Clifford, J. Ochterski, G. A. Petersson, P. Y. Ayala, Q. Cui, K. Morokuma, N. Rega, P. Salvador, J. J. Dannenberg, D. K. Malick, A. D. Rabuck, K. Raghavachari, J. B. Foresman, J. Cioslowski, J. V. Ortiz, A. G. Baboul, B. B. Stefanov, G. Liu, A. Liashenko, P. Piskorz, I. Komaromi, R. Gomperts, R. L. Martin, D. J. Fox, T. Keith, M. A. Al-Laham, C. Y. Peng, A. Nanayakkara, M. Challacombe, P. M. W. Gill, B. Johnson, W. Chen, M. W. Wong, J. L. Andres, C. Gonzalez, M. Head-Gordon, E. S. Replogle, J. A. Pople, Gaussian, Inc., Pittsburgh PA, **2002**.
[43] A. D. Becke, *J. Chem. Phys.* **1993**, *98*, 5648.
[44] C. Lee, W. Yang, R. G. Parr, *Phys. Rev. B* **1988**, *37*, 785.
[45] GaussViewW, Ver. 2.1 Gaussian Inc., **2000**.
[46] G. M. Sheldrick, SHELXL97, Program for the Refinement of Crystal Structures, University of Göttingen, Göttingen (Germany), **1997**.

Received: August 1, 2005